Since January 2020 Elsevier has created a COVID-19 resource centre with free information in English and Mandarin on the novel coronavirus COVID-19. The COVID-19 resource centre is hosted on Elsevier Connect, the company's public news and information website.

Journal of Chromatography B 1179 (2021) 122862

Contents lists available at ScienceDirect

Journal of Chromatography B

journal homepage: www.elsevier.com/locate/jchromb

Bioanalysis of niclosamide in plasma using liquid chromatography-tandem mass and application to pharmacokinetics in rats and dogs

Hae-In Choi [a,1], Taeheon Kim [b,1], Seung-Won Lee [a], Jin Woo Kim [a], Yoon Ju Noh [a], Gwan-Young Kim [b], Hyun- Jin Park [b], Yoon-Jee Chae [c], Kyeong-Ryoon Lee [d], Soo-Jin Kim [e,*], Tae-Sung Koo [a,*]

[a] Graduate School of New Drug Discovery and Development, Chungnam National University, Daejeon 34134, Republic of Korea
[b] Life Science Research Institute, Daewoong Pharmaceuticals, Yongin-si 17028, Republic of Korea
[c] College of Pharmacy, Woosuk University, Wanju-Gun 55338, Republic of Korea
[d] Laboratory Animal Resource Center, Korea Research Institute of Bioscience and Biotechnology, Ochang-eup 28116, Republic of Korea
[e] Clinical Development Division, Daewoong Therapeutics Inc., Suwon-si 16226, Republic of Korea

ARTICLE INFO

Keywords:
Niclosamide
LC-MS/MS
Pharmacokinetics
COVID-19

ABSTRACT

Niclosamide, which is an anti-tapeworm drug, was developed in 1958. However, recent studies have demonstrated the antiviral effects of niclosamide against the SARS-CoV-2 virus, which causes COVID-19. In this study, we developed and validated a quantitative analysis method for the determination of niclosamide in rat and dog plasma using liquid chromatography–tandem mass spectrometry (LC–MS/MS), and used this method for pharmacokinetic studies. Biological samples were prepared using the protein precipitation method with acetonitrile. Ibuprofen was used as an internal standard. The mobile phase used to quantify niclosamide in rat or dog plasma consisted of 10 mM ammonium formate in distilled water-acetonitrile (30:70, v/v) or 5 mM ammonium acetate–methanol (30:70, v/v). An XDB-phenyl column (5 μm, 2.1 × 50 mm) and a Kinetex® C18 column (5 μm, 2.1 × 500 mm) were used as reverse-phase liquid chromatography columns for rat and dog plasma analyses, respectively. Niclosamide and ibuprofen were detected under multiple reaction monitoring conditions using the electrospray ionization interface running in the negative ionization mode. Niclosamide presented linearity in the concentration ranges of 1–3000 ng/mL ($r = 0.9967$) and 1–1000 ng/mL ($r = 0.9941$) in rat and dog plasma, respectively. The intra- and inter-day precision values were $< 7.40\%$ and $< 6.35\%$, respectively, for rat plasma, and $< 3.95\%$ and $< 4.01\%$, respectively, for dog plasma. The intra- and inter-day accuracy values were $< 4.59\%$ and $< 6.63\%$, respectively, for rat plasma, and $< 12.1\%$ and $< 10.9\%$, respectively, for dog plasma. In addition, the recoveries of niclosamide ranged between 87.8 and 99.6% and 102–104% for rat and dog plasma, respectively. Niclosamide was stable during storage under various conditions (three freeze–thaw cycles, 6 h at room temperature, long-term, and processed samples). A reliable LC–MS/MS method for niclosamide detection was successfully used to perform pharmacokinetic studies in rats and dogs. Niclosamide presented dose-independent pharmacokinetics in the dose range of 0.3–3 mg/kg after intravenous administration, and drug exposure in rats and dogs after oral administration was very low. Additionally, niclosamide presented high plasma protein binding (>99.8%) and low metabolic stability. These results can be helpful for further developing and understanding the pharmacokinetic characteristics of niclosamide to expand its clinical use.

1. Introduction

COVID-19 is a new infectious disease caused by the severe acute respiratory syndrome coronavirus 2 (SARS-CoV-2), which emerged in December 2019 and quickly became a pandemic [1]. The structure of SARS-CoV-2, which is a single-stranded RNA coronavirus, is similar to

* Corresponding authorsat: Graduate School of Drug Discovery and Development, Chungnam National University, 99 Daehak-ro, Yuseong-gu, Daejeon 34134, Republic of Korea.(Tae-Sung Koo), Clinical Development Division, Daewoong Therapeutics Inc., 17 Daehak 4-ro, Yeongtong-gu, Suwon-si, 16226 Republic of Korea. (Soo-Jin Kim).
E-mail addresses: biopharm00@gmail.com (S.-J. Kim), kootae@cnu.ac.kr (T.-S. Koo).
[1] These authors contributed equally to this work

https://doi.org/10.1016/j.jchromb.2021.122862
Received 23 April 2021; Received in revised form 12 July 2021; Accepted 13 July 2021
Available online 18 July 2021

that of the SARS-CoV virus, which originated in China in 2002. The spike protein on the membrane surface of these viruses specifically binds to the host cell angiotensin-converting enzyme 2 receptor to rapidly penetrate and proliferate inside cells [2,3]. Typically, SARS-COV-2 is transmitted via droplets or human contact, and the infected individuals can be asymptomatic or present several respiratory infection symptoms, such as fever, cough, shortness of breath, and sore throat [4]. Recently, a few vaccines and drugs have been approved for emergency use in COVID-19 patients. Nevertheless, viral mutations occur rapidly; therefore, safe and effective drugs for COVID-19 treatment are still necessary.

Niclosamide, which is an anti-tapeworm drug, was developed in 1958. Niclosamide inhibits glucose absorption, oxidative phosphorylation, and anaerobic metabolism in tapeworms [5]. Recent studies have demonstrated that niclosamide inhibits cancer cells by blocking the WNT signaling pathway [6]. Clinical trials on niclosamide for colorectal and prostate cancers have been conducted, and the results revealed that the drug was toxic only when administered orally in high doses [7–9]. Furthermore, studies have demonstrated the antiviral effects of niclosamide against MERS-CoV, SARS-CoV, and SARS-CoV-2 at cellular level via autophagy activation through inhibition of the SKP2 signaling pathway [10–12]. In addition, according to a recent study on 48 drugs previously approved by the US Food and Drug Administration (FDA) for SARS-CoV-2, niclosamide was approximately 40 times more effective than antiviral drugs, such as remdesivir and chloroquine, at cellular level [13]. Moreover, clinical studies on COVID-19 treatments are in progress in the USA, Germany, Australia, and Korea [14].

Many reports regarding the pharmacological effects and clinical results of niclosamide, which is an old drug, have been published. However, information on analytical methods used for niclosamide detection in biological samples and pharmacokinetic analysis in animals is limited. Doran and Stevens [15] and Jiang et al. [16] used liquid chromatography–tandem mass spectrometry (LC–MS/MS) for niclosamide detection in water; however, the proposed methods could not be extrapolated to the analysis of biological matrices in general or plasma samples in particular. Chang et al. [17] studied the pharmacokinetics of niclosamide in rats; however, the sensitivity, precision, accuracy, and matrix effect of their method for biological samples has not been validated. In addition, because their study compared simple pharmacokinetic results with other derivatives, evaluating the pharmacokinetic properties of niclosamide was limited.

In this study we developed and validated a quantitative analysis method for the determination of niclosamide in rat and dog plasma using a LC–MS/MS system in accordance with the European Medicines Agency (EMA) and US FDA guidelines. Furthermore, we used the developed method to perform pharmacokinetic studies to evaluate the *in vitro* and *in vivo* mechanisms of niclosamide.

2. Material and methods

2.1. Materials

Niclosamide (lot No. 140001Y01A, Derivados Quimicos, Murcia, Spain) was provided by Daewoong Therapeutics Inc. (Suwon, Korea). Ibuprofen (Cat. No. I4883), which was used as an internal standard (IS), dimethyl sulfoxide (DMSO; Cat. No. D2660), and ammonium acetate (Cat. No. A1542) were purchased from Sigma-Aldrich (St. Louis, MO, USA). High-performance liquid chromatography (HPLC)-grade water (Cat. No. 4218–88), acetonitrile (Cat, No. UN1648), and methanol (Cat. No. AH230-4) were obtained from J.T. Baker (Phillipsburg, NJ, USA). Ammonium formate (Cat. No. 25030–0401, Juncei Chemical, Tokyo, Japan), sodium hydroxide (NaOH; Cat No. 7576–3700, Daejung Chemicals, Siheung, Korea), polyethylene glycol-400 (PEG 400; Cat No. P0638, Samchun Chemicals, Pyeongtaek, Korea), carboxymethyl cellulose (CMC; Lot No. 76757, Ashland, OR, USA), and all other chemicals used in this study were of analytical grade. Heparinized rat and dog plasma samples were prepared in house and were obtained from Knotus (Incheon, Korea), respectively.

2.2. Analytical procedure

All biological samples, except the dog-derived samples, were analyzed under the following LC–MS/MS conditions. We used an Agilent 1100 (Agilent Technologies, Santa Clara, CA, USA) HPLC system with a Zorbax Eclipse XDB-Phenyl (5 μm, 2.1 × 50 mm, Agilent, Santa Clara, CA, USA) column connected to a Zorbax Eclipse XDB-C8 (5 μm, 2.1 × 12.5 mm, Agilent, Santa Clara, CA, USA) guard column, which was used as the reverse-phase column and was maintained at 40 °C. The mobile phase consisted of a mixture of 10 mM ammonium formate-acetonitrile 30:70 (v/v), and separation occurred via isocratic elution at a flow rate of 0.3 mL/min with an injection volume of 5 μL. The autosampler temperature was maintained at 10 °C. All analytes were detected using an API 4000 QTrap (AB Sciex, Framingham, MA, USA) triple quadrupole mass spectrometer in the negative ionization mode of the electrospray ionization (ESI) interface. The MS parameters were as follows: ion voltage of − 4200 V, temperature of 600 °C, curtain gas pressure of 20 psi, nebulizer gas pressure of 50 psi, turbo gas pressure of 50 psi, entrance potential of − 10 V, declustering potentials of −55 and −45 V, collision energies of − 38 and − 10 V, and collision cell exit potentials of − 11 and − 1 V for niclosamide and ibuprofen, respectively. The multiple reaction mode (MRM) was used to quantify the ion transitions at *m/z* 324.8 → 170.9 and 205.0 → 161.1 for niclosamide and ibuprofen, respectively. The peak areas were integrated automatically using the Analyst software version 1.6.2 (Applied Biosystems/MDS SCIEX, Framingham, MA, USA).

Dog plasma samples were analyzed using the following LC–MS/MS conditions. We used an Exion (AB Sciex, Framingham, MA, USA) HPLC system with a Kinetex® C18 (5 μm, 2.1 × 500 mm, Phenomenex, Torrance, CA, USA) reverse phase column, which was maintained at 25 °C. The autosampler temperature was maintained at 4 °C. The mobile phase consisted of 5 mM ammonium acetate–methanol 30:70 (v/v) and separation occurred via isocratic elution at a flow rate of 0.2 mL/min with an injection volume of 2 μL. All analytes were detected using a Triple Quad 6500 (AB Sciex, Framingham, MA, USA) LS–MS/MS system in the negative ionization mode of the ESI interface. The MS parameters were as follows: ion voltage of − 4500 V, temperature of 550 °C, curtain gas pressure of 40 psi, nebulizer gas pressure of 50 psi, turbo gas pressure of 50 psi, entrance potential of − 10 V, declustering potentials of − 45 and − 60 V, collision energies of − 34 and − 10 V, and collision cell exit potential of − 11 V for niclosamide and ibuprofen, respectively. The MRM was used to quantify the transitions at *m/z* 325.0 → 170.9 and 205.0 → 161.1 for niclosamide and ibuprofen, respectively. The peak areas were integrated automatically using the Analyst software version 1.6.2 (Applied Biosystems/MDS SCIEX, Framingham, MA, USA).

2.3. Sample preparation

To make the standard sample for the calibration curve, 10-fold concentrated working standard solution was prepared via serial dilution of niclosamide with acetonitrile, and the working standard solution for QC samples were independently prepared.

For rat plasma samples, 20 μL of acetonitrile containing IS (1 μg/mL of ibuprofen) and 160 μL of acetonitrile were added to 20 μL of a rat plasma to induce protein precipitation. Thereafter, the mixture was vigorously mixed for 10 min, followed by centrifugation at 13500 rpm for 10 min. Next, the supernatant was transferred into a vial, and 5 μL of supernatant was injected into the LC–MS/MS system.

For dog plasma samples, 200 μL of acetonitrile containing IS were added to 50 μL of a dog plasma to induce protein precipitation. After mixing and centrifugation in the same manner as in the rat, 20 μL of supernatant was further diluted 10 times with the mobile phase, and then 2 μL of the supernatant was injected into the LC-MS/MS system.

2.4. Method validation

The method validation parameters, namely specificity, linearity, precision and accuracy, matrix effect, recovery, process efficiency, and stability were analyzed according to the guidelines of the EMA and US FDA [18,19].

Specificity was evaluated using six lots of untreated blank plasma samples, and the results were compared with those of the respective analyte and IS-spiked samples. The retention times of the analyte and IS were compared to confirm the absence of interference peaks of endogenous substances in plasma. The calibration curves of niclosamide in plasma were obtained by plotting the peak ratios of niclosamide to ibuprofen *vs.* the nominal concentrations of the calibration standards (1, 2, 5, 10, 30, 100, 300, 1000, 2000, and 3000 ng/mL for rats, or 1, 3, 10, 30, 100, 300, and 1000 ng/mL for dogs). Calibration curves were fitted using least-squares linear regression analysis using a weighted factor ($1/x^2$). Linearity was validated using correlation coefficients (r).

The precision and accuracy of the analytical method were validated using the lower limit of quantification (LLOQ; 1 ng/mL) and QC samples (3, 500, and 2700 ng/mL for rats and 2.5, 50, and 500 ng/mL for dogs). Precision was expressed as the coefficient of variation (CV%), which was obtained as the percentage of the standard deviation (SD) of the peak area ratio divided by the mean of the peak area ratio of niclosamide and IS. The accuracy was calculated as the relative error (%RE), which was obtained as the percentage of the difference between the measured and nominal concentrations divided by the nominal concentrations of niclosamide. The intra-day precision and accuracy of the analytical method were determined by repeating experiments five times per day, whereas the inter-day precision and accuracy of the analytical method were obtained by repeating experiments for 3 day.

The matrix effect, recovery, and process efficiency were measured for each QC group. A matrix effect experiment was performed to evaluate the enhancement or suppression of analyte ionization owing to the presence of matrix components in the samples. The matrix effect was calculated by dividing the mean of the peak areas of niclosamide spiked in a blank plasma extract (set 2) by the peak area of the analyte added using the mobile phase of the clean analyte solutions (set 1). Recovery was estimated by comparing the mean peak areas of the analyte in the sample extracts (set 3) with those of the samples in set 2. Process efficiency was calculated by comparing the data for sets 1 and 3 [20,21].

Sample stability was determined at low and high QC concentrations. Short-term stability was evaluated at room temperature for 6 h, whereas processed sample stability was evaluated by comparison with samples prepared using an autosampler at 10 °C for 24 h. Long-term stability was determined by assaying samples stored at −20 °C for four weeks and samples that underwent three freeze–thaw cycles.

2.5. In vitro studies

2.5.1. Plasma protein binding assay

An equilibrium dialysis device (RED®, Thermo, Waltham, MA, USA) was used to perform the plasma protein binding assay of niclosamide in rats, dogs, and humans. A semi-permeable membrane was used to separate the chamber containing plasma spiked with 2 μg/mL of niclosamide from that containing phosphoric acid buffer (pH 7.4). Incubation was performed in a water bath shaken for 4 h at 100 rpm and 37 °C. Thereafter, 50 μL aliquots from each chamber were collected, pretreated, and analyzed using LC–MS/MS. Plasma protein binding was calculated as follows: 1 − (concentration in buffer/concentration in plasma).

2.5.2. Microsomal stability

The metabolic stability of niclosamide was examined using rat, dog, and human liver microsomes. Niclosamide was dissolved in DMSO and diluted to final niclosamide concentrations of 1 μM. Reactions were performed in triplicate in 96-well plates at a final volume of 160 μL in 0.1 M potassium phosphate buffer and 0.5 mg/mL of rat, dog, and human liver microsomes. The plates were incubated at 37 °C before a 1 mM β-nicotinamide adenine dinucleotide phosphate solution was added to each well. The reaction was terminated at 0, 10, 30, and 60 min by adding 320 μL of ice-cold acetonitrile containing IS to the wells. The samples were centrifuged at 3000 rpm for 10 min. The supernatant (5 μL) was analyzed using an LC–MS/MS system in the MRM mode. Subsequently, hepatic clearance (CL_H) was estimated using the *in vitro* intrinsic clearance ($CL_{int,\ in\ vitro}$) levels in liver, which was calculated using the metabolic stability data and following equations [20]:

$$T_{1/2} = -ln2/k_e \tag{1}$$

$$CL_{int,in\ vitro} = k_e \times (mL\ incubation/mg\ microsomes) \tag{2}$$

$$CL_{u,int,\ vivo} = f_{u\ mic} \times CL_{u,int,\ vivo} \times (45\,mg\ microsomes/g\ liver) \times (g\ liver/kg\ body\ weight) \tag{3}$$

and

$$CL_H = f_{ub} \times CL_{u,int,in\ vivo} \times Q_h/\left(f_{ub} \times CL_{u,int,in\ vivo} + Q_h\right) \tag{4}$$

where $T_{1/2}$, k_e, $f_{u\ mic}$, f_{ub}, $CL_{u\ int\ in\ vivo}$, and Q_h denote the elimination half-life, elimination rate constant, microsome- and blood-unbound fraction of niclosamide, *in vivo* intrinsic clearance, and hepatic blood flow, respectively. To calculate f_{ub}, the plasma unbound fraction was divided by the blood-to-plasma concentration ratio and then multiplied by (1–0.44), and $f_{u\ mic}$ was assumed to be 0.5.

2.6. In vivo pharmacokinetic studies

Male Sprague Dawley (SD) rats (7 weeks old) weighing 210–251 g were purchased from Orient Bio Inc. (Seongnam, Korea). Their habitat was maintained under a 12 h light–dark cycle at a temperature of 20–25 °C and relative humidity of 40–60%. Rats fasted for 14 h before and 4 h after drug administration. Studies on rats were approved in advance by the Institutional Animal Care and Use Committee of Chungnam National University (202003A-CNU-055; Daejeon, Korea). Niclosamide dosing solutions with concentrations of 0.15, 0.5, and 1.5 mg/mL were prepared using a mixture of 10% DMSO, 30% PEG, 20% of a 0.05 N NaOH solution, and 40% saline as the solvent. Thereafter niclosamide was administered to the rats via a single intravenous (IV) bolus injection into the tail vein (0.3, 1, and 3 mg/kg), orally (PO) using a gavage needle (1 mg/kg), or via intramuscular injection (IM) into the thigh (1 mg/kg). Blood samples (150 μL) were collected from the jugular vein using heparinized syringes at 0.083 (IV and IM only), 0.25, 0.5, 1, 2, 4, 6, 8, and 24 h after dosing. All blood samples were centrifuged, and 20 μL plasma aliquots were frozen at − 20 °C before they were subjected to LC–MS/MS analysis.

Pharmacokinetic studies in beagle dogs were performed at Knotus (Incheon, Korea). Male Beagle dogs, aged 10–12 months old and weighting 7.3–9.7 kg, were purchased from Orient Bio Inc. (Jeongeup, Korea). Their habitat was maintained under a 12 h light–dark cycle at a temperature of 23 ± 3 °C and relative humidity of 55 ± 15%. All dogs fasted for 14 h before and 4 h after niclosamide administration. An IV niclosamide dosing solution with a concentration of 2 mg/mL was prepared using a mixture of 10% DMSO, 30% PEG, 20% of a 0.05 N NaOH solution, and 40% saline as the solvent, and a PO niclosamide dosing solution with a concentration of 20 mg/mL was prepared using 1% CMC as the solvent. Thereafter, niclosamide was administered to the dogs via a single IV bolus injection into the cephalic vein (2 mg/kg) or PO using a gavage needle (100 mg/kg). Blood samples (3 mL) were collected from the jugular vein using heparinized syringes at 0.083 (IV only), 0.25, 0.5, 1, 2, 4, 6, 8, and 24 h after dosing. All blood samples were centrifuged, and 50 μL plasma aliquots were frozen at − 20 °C before LC–MS/MS analysis.

The Phoenix® 8.2 (Certara L.P., Princeton, NJ, USA) software was

used to calculate the pharmacokinetic parameters, as follows. k_e was determined using the linear regression of the log-linear portion of the terminal phase; $T_{1/2}$ was calculated using Eq. (1); the elimination clearance (CL), steady-state volume of distribution (V_{ss}), and mean residence time (MRT) were determined via moment analysis; and the absorption constant (k_a) was calculated as follows: $k_a = 1/MRT_{po} - MRT_{iv}$ [22,23]. The area under the concentration of niclosamide in plasma *vs.* time curve in the 0 to ∞ time interval (AUC_{inf}) was calculated using the linear trapezoidal rule and standard area extrapolation method. The maximum plasma concentration (C_{max}) and time C_{max} was reached (T_{max}) were determined directly from the plasma concentration–time curves.

2.7. Statistics

All data are reported as mean ± SD. The pharmacokinetic parameters were estimated using one-way analysis of variance (ANOVA) and the Prism 7.0 (GraphPad Software, San Diego, CA, USA) software. A result was considered statistically significant when $p < 0.05$ for both analyses.

3. Results and discussion

3.1. Development of the LC–MS/MS method

The niclosamide and ibuprofen ions were detected using MRM conditions. The deprotonated precursor ions of niclosamide and ibuprofen

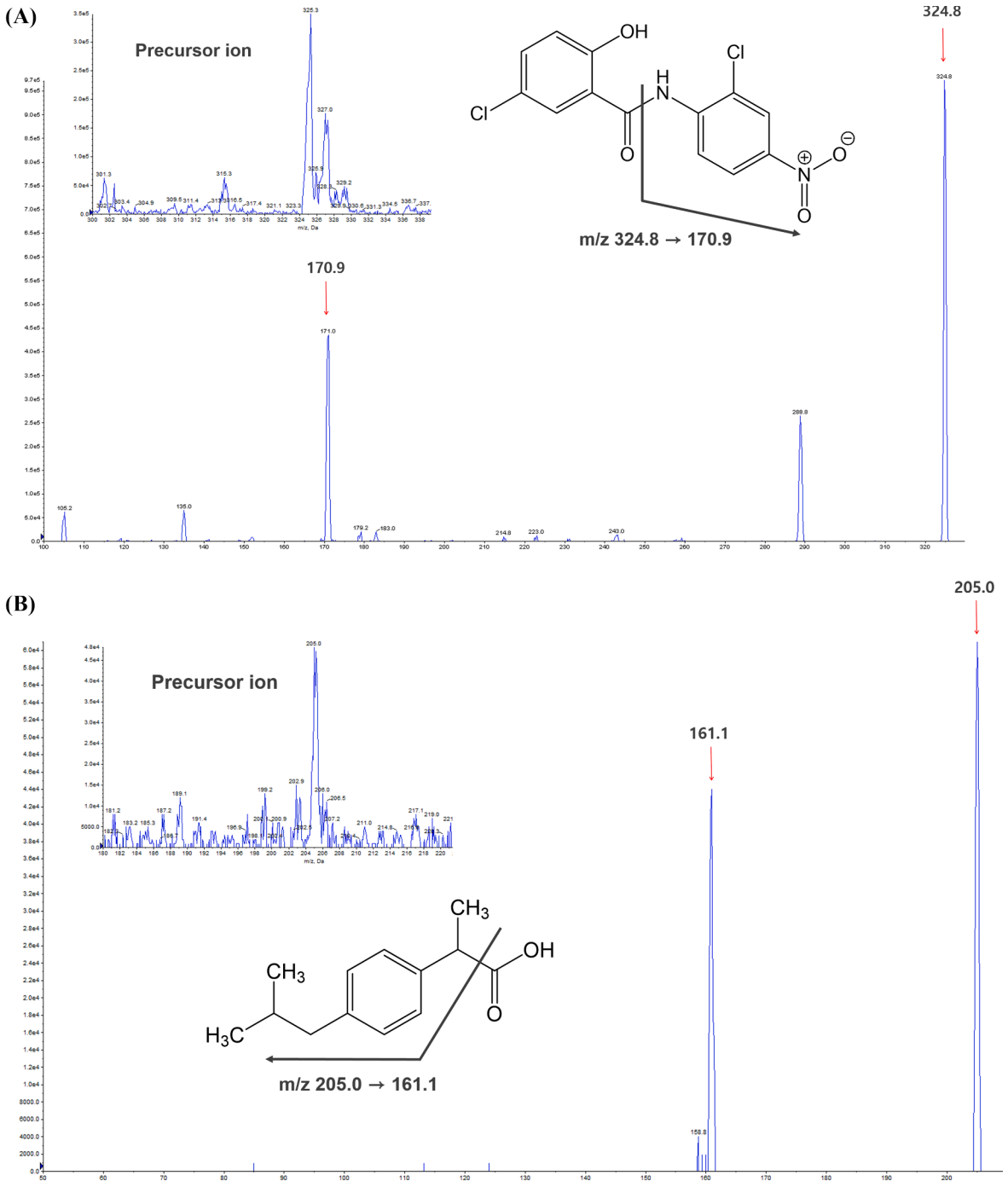

Fig. 1. Product ion mass spectra of (A) niclosamide and (B) ibuprofen.

([M−H]$^-$) were detected at m/z of 324.8 and 205.0, respectively, using the negative ionization mode of the ESI interface in the Q1 scan spectra. The transitions of the product ions of niclosamide were observed at m/z 324.8 → 170.9 and 324.8 → 288.8 with negligible difference in sensitivity; however, the m/z 324.8 → 170.9 transition was selected because it presented better linearity, which was similar to that previously reported [15,16]. Niclosamide molecules contain two Cl atoms, with a ^{35}Cl-to-^{37}Cl ratio of 3:1. The typical Cl isotope ratio of molecules containing two Cl atoms is approximately 9:6:1. When the precursor ion was analyzed using the Q1 scan, three isotope peaks at a ratio of approximately 9:6:1 were observed in the profile of niclosamide [15]. For ibuprofen (the IS), the transition of product ions was observed at m/z 205.0 → 161.1 (Fig. 1).

The mobile phase and column conditions were changed to optimize

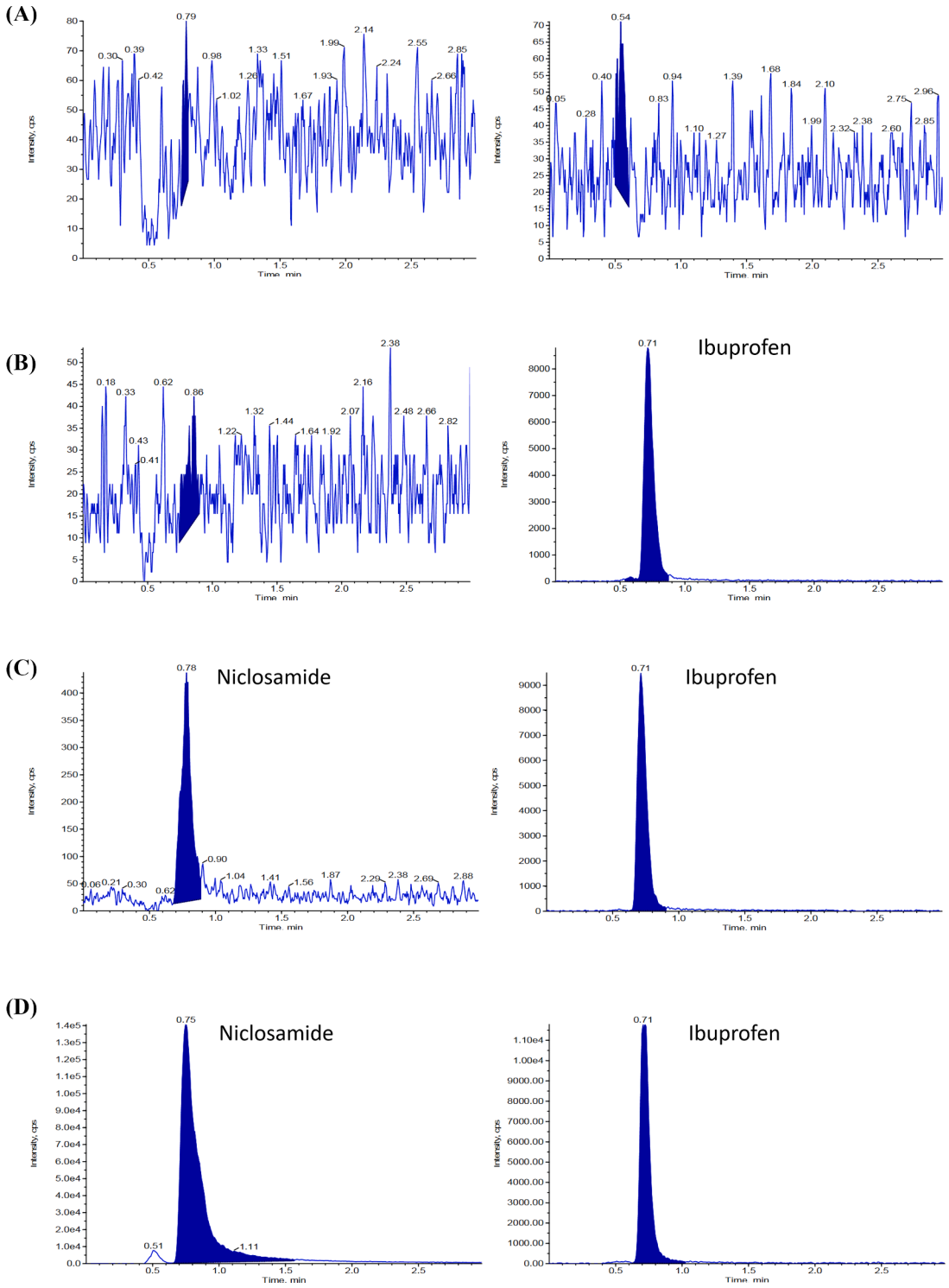

Fig. 2. Liquid chromatography–tandem mass spectrometry chromatograms of niclosamide and ibuprofen in rat and dog plasma. (A) Blank rat plasma, (B) rat plasma with 1000 ng/mL ibuprofen only, (C) rat plasma containing 1 ng/mL niclosamide and 1000 ng/mL ibuprofen, (D) plasma samples collected 15 min after intravenous administration of 1 mg/kg niclosamide to rats, (E) blank dog plasma, (F) dog plasma with 1000 ng/mL ibuprofen only, (G) dog plasma containing 1 ng/mL niclosamide and 1000 ng/mL ibuprofen, and (H) plasma samples collected 2 h after intravenous administration of 2 mg/kg niclosamide to dogs.

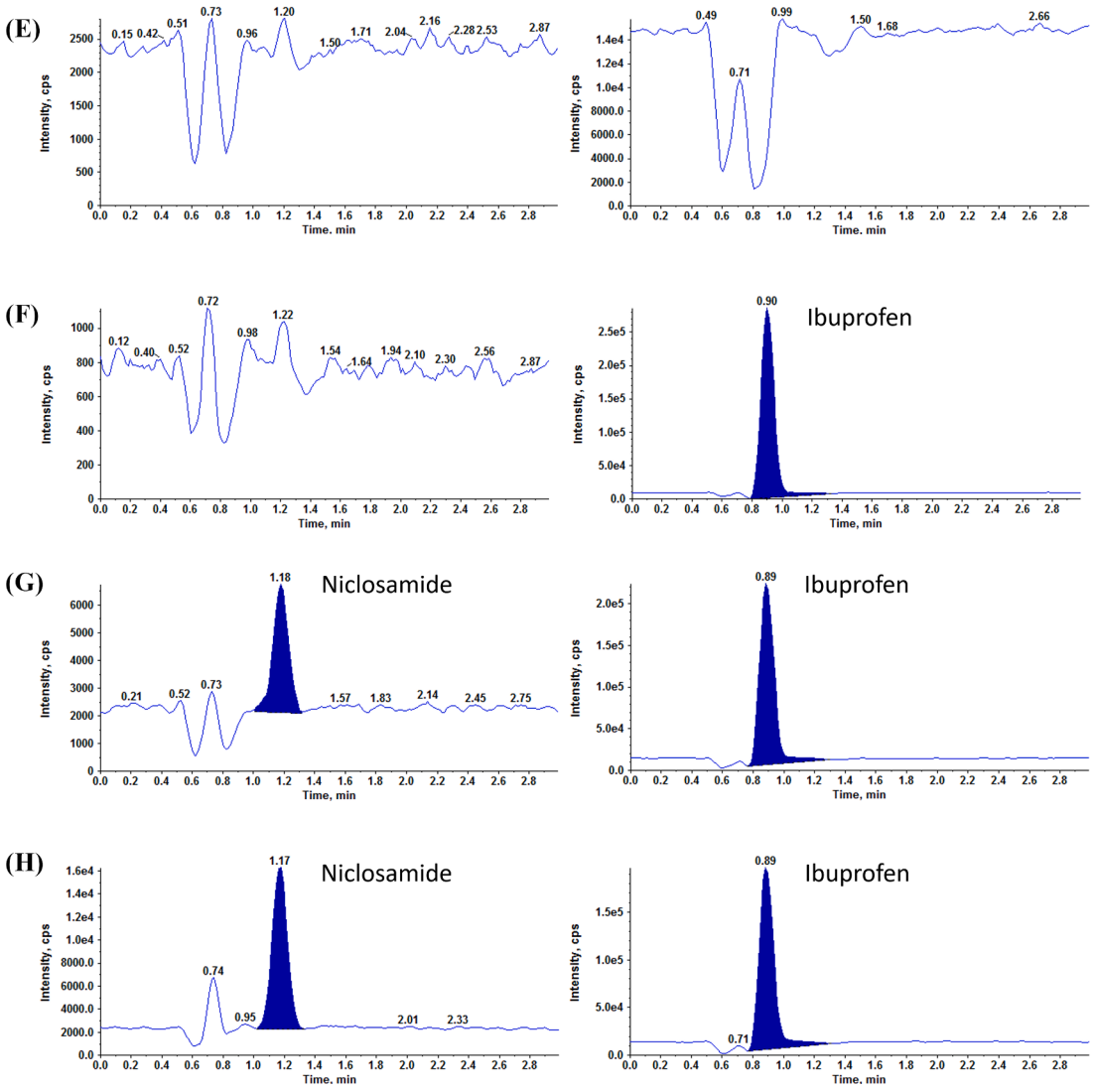

Fig. 2. (*continued*).

the plasma chromatograms. To detect niclosamide in rat plasma using the API 4000 QTrap spectrometer, we used a mixture of 10 mM ammonium formate-acetonitrile (30:70 v/v) as the mobile phase. These solvents are commonly used in the negative ion mode of the ESI interface because weak base conditions favor ionization. Consequently, the sensitivity was higher than that when 0.1% formic acid was used as the mobile phase, allowing niclosamide quantification at lower concentrations. The performance of the commonly used C18 and Phenyl columns in the API 4000 QTrap spectrometer was compared. The sensitivity of the XBD-C18 (Agilent, Santa Clara, CA) column was approximately twice as high that of the XBD-Phenyl column (Agilent, Santa Clara, CA); however, the XBD-Phenyl column was selected owing to its low baseline, adequate quantification range, peak shape, and negligible carryover in rat plasma (Fig. 2A-D). Niclosamide in dog plasma samples was detected using a QTrap 6500 LC–MS/MS system with a higher sensitivity than the API 4000 QTrap spectrometer used for rat plasma analysis. When the same method used for rat plasma analysis was utilized for dog plasma samples, an interference peak was observed in the chromatogram of blank plasma. Therefore, a Kinetex® C18 (5 μm, 2.1 × 500 mm) column and 5 mM ammonium acetate–methanol (30:70, v/v) mobile phase were used to improve peak shape and analyte separation in dog plasma samples (Fig. 2E-H).

3.2. Method validation

Because the analyte signal was more than five times stronger that of the blank sample, 1 ng/mL was considered to be the LLOQ for both rat and dog plasma. The LC–MS/MS retention times of niclosamide and ibuprofen were 0.77 and 0.71 min for rat plasma and 1.18 and 0.85 min for dog plasma, respectively; moreover, a constant retention time was observed during repeated experiments, enabling a reproducible and reliable analysis without interference from endogenous substances in both types of plasma samples. In addition, this method did not present a carryover effect. The chromatograms of the blank sample (without analyte or IS), LLOQ (1 ng/mL), and plasma samples after niclosamide administration to rats and dogs are presented in Fig. 2.

The calibration curve for niclosamide, which was obtained using five rat plasma samples, namely blank plasma, zero, and calibration standard samples, presented a good linearity in the concentration range of 1–3000 ng/mL ($r = 0.9967$). The equation of the standard curve for niclosamide: $y = 0.0391x + 0.0119$, was obtained using a weighting factor of $1/x^2$. The calibration standard curve for niclosamide in dog plasma samples presented a good linearity in the range of 1–1000 ng/mL ($r = 0.9941$), and the equation of the standard curve was $y = 0.01600x + 0.001667$. Dilution integrity was validated for concentrations up to 10 times higher than the high QC concentration in five replicates; moreover, CV was 4.54%, and RE was − 2.48%.

The precision and accuracy values of the method are summarized in Table 1. For rat plasma, the intra- and inter-day precision values were < 7.40% and < 6.35%, respectively, whereas the intra- and inter-day accuracy values were < 4.59% and < 6.63%, respectively, at four concentration levels (lower quality control, middle quality control, and higher quality control concentrations, and LLOQ). For dog plasma, the intra- and inter-day precision values were < 5.55% and < 5.82%, respectively, and the intra- and inter-day accuracy values were < 13.0% and < 12.7%, respectively. These results satisfied the acceptance criteria [18,19] and demonstrated that the method used to analyze rat and dog plasma samples was reproducible and reliable.

The matrix effect, recovery, and process efficiencies of niclosamide and IS in both types of plasma samples were determined at three QC sample concentrations. For rat plasma, the matrix effect ranged between 73.8 and 87.7% (IS, 81.4%), recovery ranged between 87.8 and 99.6% (IS, 89.0%), and process efficiency ranged between 72.6 and 87.2% (IS, 72.4%). If the samples were normalized with IS, the matrix effect, recovery, and process efficiency were improved by 100–108%. For dog plasma, the matrix effect ranged between 94.9 and 102% (IS, 94.8%), recovery ranged between 102 and 104% (IS, 79.1%), and process efficiency ranged between 98.1 and 104% (IS, 75.0%). These results suggested that protein precipitation was an appropriate pretreatment for efficient niclosamide and ibuprofen extraction from rat and dog plasma.

The stability values of niclosamide in rat and dog plasma are summarized in Table 2. Niclosamide in rat and dog plasma samples was stable at room temperature for 6 h, for three freeze–thaw cycles, in an autosampler at 10 °C for 24 h, and at − 20 °C for one month.

3.3. In vitro studies

Owing to plasma protein binding through equilibrium dialysis, niclosamide in rat, dog, and human plasma samples presented high plasma protein bindings of 99.86 ± 0.006%, 99.83 ± 0.015%, and 99.84 ± 0.042%, respectively; these values were not significantly different.

The mean residual concentration–time profiles of niclosamide in rat, dog, and human hepatic microsomes are presented in Fig. 3. Owing to its stability in rat, dog, and human liver microsomes, a 1 μM niclosamide solution was incubated for 60 min, and 39.7%, 7.49%, and 2.95%, respectively, of the initial niclosamide amount was recovered. The half-lives of niclosamide in rat, dog, and human hepatic microsomes were 44.9, 16.0 and 11.8 min, respectively. These results indicated that niclosamide was metabolically unstable with a half-life of 45 min, and the half-life was shorter in larger mammals. The estimated k_e, $CL_{int,\ in\ vitro}$, and CL_H values in rat liver microsomes were 0.015 min^{-1}, 6661 mL/(h·kg), and 12.1 mL/(h·kg), respectively. For dog liver microsomes, k_e, $CL_{int,\ in\ vitro}$, and CL_H were 0.043 min^{-1}, 25841 mL/(h·kg), and 45.9 mL/(h·kg), respectively; and for human liver microsomes, k_e, $CL_{int,\ in\ vitro}$, and CL_H were 0.059 min^{-1}, 17980 mL/(h·kg), and 31.9 mL/(h·kg), respectively. The estimated *in vitro* CL_H values were compared with the CL values of the *in vivo* study, and the clearance scaling factors in rats and dogs were determined to be approximately 86.0 and 54.4, respectively. Using the scaling factors for rat and dog liver microsomes, it was estimated that CL for human liver microsomes ranged between 1735 and 2743 mL/(h·kg). In addition, the significant difference between *in vitro* CL_H and *in vivo* CL values (12.1 *vs.* 1041 mL/(h·kg) for rat liver microsomes and 45.9 *vs.* 2496 mL/(h·kg) for dog liver microsomes) indicated that the major elimination route of niclosamide was not phase 1

Table 1
Intra- and inter-day precision and accuracy values.

(A) Rat plasma			
Spiked concentration (ng/mL)	Measured concentration (ng/mL)	Precision (% CV)	Accuracy (% RE)
Intra-day (n = 5)			
1	0.996 ± 0.041	4.135	−0.380
3	2.888 ± 0.214	7.400	−3.733
500	514.6 ± 34.30	6.666	2.920
2700	2576 ± 98.39	3.819	−4.593
Inter-day (n = 15)			
1	1.002 ± 0.047	4.705	0.173
3	3.057 ± 0.194	6.346	1.889
500	533.1 ± 21.25	3.985	6.627
2700	2682 ± 159.6	3.819	−4.593
(B) Dog plasma			
Spiked concentration (ng/mL)	Measured concentration (ng/mL)	Precision (% CV)	Accuracy (% RE)
Intra-day (n = 5)			
1	1.130 ± 0.043	3.806	13.00
2.5	2.624 ± 0.146	5.553	4.960
50	48.52 ± 1.612	3.321	−2.960
500	461.8 ± 10.83	2.344	−7.640
Inter-day (n = 15)			
1	1.127 ± 0.049	4.377	12.73
2.5	2.655 ± 0.143	5.389	6.187
50	49.51 ± 2.156	4.354	−0.973
500	485.1 ± 28.21	5.816	−2.987

Table 2
Niclosamide stability in rat and dog plasma.

(A) Rat plasma		
Storage conditions (n = 4)	Spiked concentration (ng/mL)	Stability in rat plasma (%)
Processed sample	3	95.68 ± 6.310
	2700	100.0 ± 2.067
6 h at RT	3	100.1 ± 7.333
	2700	98.40 ± 3.349
1 month at − 20 ℃	3	96.68 ± 7.883
	2700	95.17 ± 1.712
Three freeze–thaw cycles	3	104.7 ± 8.505
	2700	98.80 ± 3.323
(B) Dog plasma		
Storage conditions (n = 5)	Spiked concentration (ng/mL)	Stability in dog plasma (%)
Processed sample	2.5	97.84 ± 3.436
	500	87.12 ± 0.955
6h at RT	2.5	101.6 ± 3.837
	500	90.60 ± 3.450
1 month at −20 ℃	2.5	96.88 ± 8.501
	500	90.08 ± 2.838
Three freeze–thaw cycles	2.5	95.44 ± 2.920
	500	93.64 ± 3.474

Processed sample, 10 °C autosampler for 24 h; RT, room temperature; freeze–thaw cycles, −80 °C → RT.

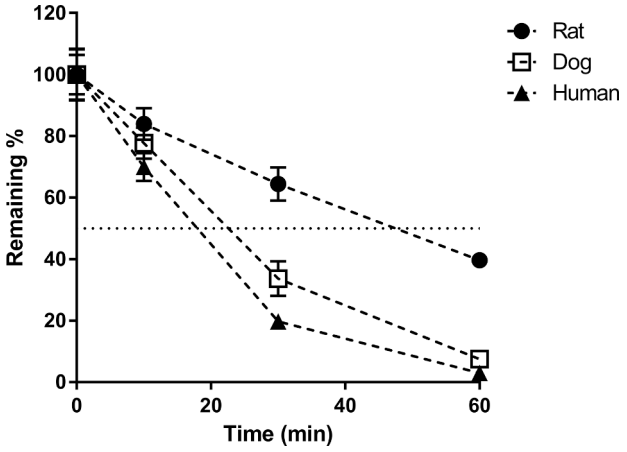

Fig. 3. Residual niclosamide levels (%) in (●) rat, (□) dog, and (▲) human hepatic microsomes. Each data point represents the mean ± SD. (n = 3).

metabolism mediated by CYP enzymes. Additionally, it was confirmed that the half-life of niclosamide was approximately 10 times shorter when the microsomes were treated with uridine diphosphate glucuronic acid, indicating that phase 2 metabolism studies should be performed (data not included).

3.4. In vivo pharmacokinetic studies

The mean plasma concentration–time profiles of niclosamide after IV (0.3, 1, and 3 mg/kg), PO (1 mg/kg), and IM (1 mg/kg) administration to rats are presented in Fig. 4A. The mean plasma concentration–time profiles of niclosamide after IV (2 mg/kg) and PO (100 mg/kg) administration to dogs are illustrated in Fig. 4B. The pharmacokinetic parameters of niclosamide in rats and dogs are summarized in Table 3.

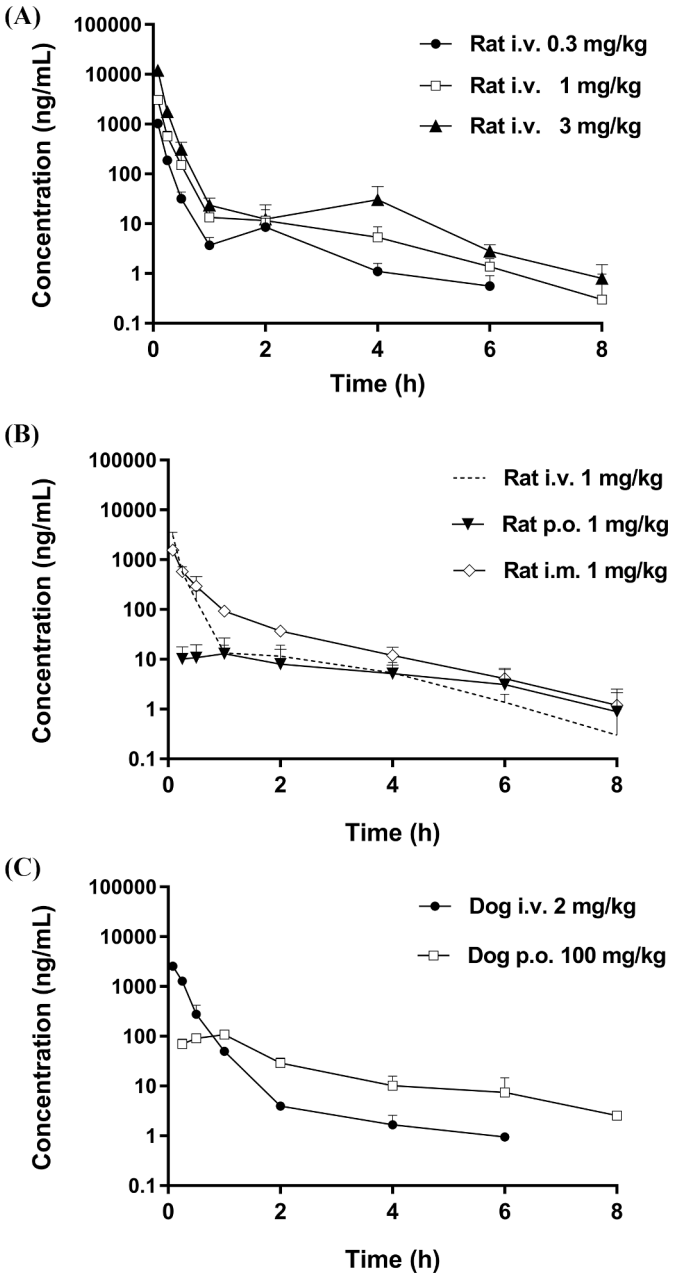

Fig. 4. Plasma concentration–time curves after (A) intravenous (0.3 mg/kg, ●; 1 mg/kg, □; and 3 mg/kg, ▲) administration and (B) intravenous (1 mg/kg, dotted line), oral (1 mg/kg, ▼), and intramuscular (1 mg/kg, ◇) administration of niclosamide to Sprague Dawley rats and (C) intravenous (2 mg/kg, ●) and oral (100 mg/kg, □) administration of niclosamide to beagle dogs. Each data point represents the mean ± SD. (n = 5 for rats and n = 3 for dogs).

After IV administration of 0.3, 1, and 3 mg/kg niclosamide to rats, C_{max} was 1035 ± 166, 3088 ± 481, and 11920 ± 1144 ng/mL, respectively, at the first sampling time (0.083 h), and AUC_{last} was 301 ± 49.2, 903 ± 150, and 3375 ± 254 ng·h/mL, respectively. This indicated that upon increasing the niclosamide nominal dose by 3.3 and 10 times, C_{max} and AUC_{last} increased in a dose-dependent manner, namely 3.0 and 11.5 times for C_{max} and 3.0 and 11.2 times for AUC_{last}. Furthermore, the CL values at the niclosamide doses of 0.3, 1, and 3 mg/kg were 1012 ± 164, 1130 ± 188, and 892 ± 66.9 mL/(h·kg), respectively, which were moderate compared with the hepatic blood flow rate of rats (3300 mL/(h·kg)) [23], and did not change significantly with the niclosamide dose. The V_{ss} value was low < 400 mL/kg in the niclosamide dose range of 0.3–3 mg/kg. This suggested that niclosamide was confined mainly to the plasma pool with limited tissue distribution because of its high plasma protein-binding properties. The one-way ANOVA results indicated that the $T_{1/2}$, MRT, CL, and V_{ss} values were not significantly different ($p > 0.05$) with increasing niclosamide dose, and the pharmacokinetic properties were dose-independent in the niclosamide dose range of 0.3–3 mg/kg.

Pharmacokinetic studies for different administration routes were performed by administering single IV, PO, and IM doses of 1 mg/kg niclosamide to SD rats. The k_a value was calculated to be 0.34 h^{-1} using the following equation [22]: $k_a = 1/MRT_{po} - MRT_{iv}$; k_a was lower than k_e (0.70 h^{-1}), which was estimated through linear regression analysis, suggesting that niclosamide presented flip-flop kinetics. The oral bioavailability of niclosamide in rats was 5.51 ± 1.02% and plasma exposure was very low, indicating that absorption was limited considering that the CL value was moderate compared with the hepatic blood flow rate of rats. The IM absorption rate of niclosamide in rats was high with a T_{max} of 5 min, and bioavailability was higher than that achieved via PO administration.

For dogs, after IV administration of 2 mg/kg of niclosamide, a C_{max} of 2543 ± 386 ng/mL was achieved 5 min after administration; furthermore, the mean CL value was 2496 ± 360 mL/(h·kg). Considering that the liver blood flow of dogs was 1860 mL/(h·kg) [23], the mean CL was high. The mean V_{ss} value was low (661 ± 61.7 mL/kg), indicating that niclosamide was not well distributed in tissues. For a single PO dose of 100 mg/kg of niclosamide, C_{max} and T_{max} were 109 ± 14.0 ng/mL and 0.833 ± 0.290 h, respectively, and absorption rate was moderate. Moreover, $T_{1/2}$ was moderate (~1.03 ± 0.89 and 1.66 ± 0.17 h after IV and PO administration, respectively). Flip-flop kinetics were also observed for dogs, indicating that the absorption rate was lower than the elimination rate. The oral bioavailability of niclosamide (0.54%) was very low and was ascribed to the high CL value.

4. Conclusions

In conclusion, a reliable LC–MS/MS method for the detection of niclosamide in rat and dog plasma was proposed. The method was in line with the US FDA and EMA guidelines and was successfully used for pharmacokinetic studies. Niclosamide presented linear pharmacokinetics in an IV dose range of 0.3–3 mg/kg in rats; moreover, drug exposure in rats and dogs following PO administration was very low. In addition, niclosamide presented a low metabolic stability in rat, dog, and human liver microsomes. These results can be helpful for further developing and understanding the pharmacokinetic characteristics of niclosamide to expand its clinical use.

CRediT authorship contribution statement

Hae-In Choi: Formal analysis, Writing - original draft. **Taeheon Kim:** Formal analysis. **Seung-Won Lee:** Formal analysis. **Jin Woo Kim:** Formal analysis. **Yoon Ju Noh:** Formal analysis. **Gwan-Young Kim:** Investigation, Data curation. **Hyun- Jin Park:** Investigation, Data curation. **Yoon-Jee Chae:** Investigation, Data curation, Writing - review

Table 3
Pharmacokinetic (PK) parameters of niclosamide after intravenous, oral, and intramuscular administration to rats and dogs.

PK Parameter	Sprague Dawley Rat					Beagle Dog	
	Intravenous			Oral	Intramuscular	Intravenous	Oral
Dose (mg/kg)	0.3	1	3	1	1	2	100
T_{max} (h)	0.083 ± 0.000	0.083 ± 0.000	0.083 ± 0.000	0.950 ± 0.671	0.083 ± 0.000	0.083 ± 0.000	0.830 ± 0.290
C_{max} (ng/mL)	1035 ± 166.4	3088 ± 480.5	11920 ± 1144	22.42 ± 7.992	1566 ± 97.88	2543 ± 385.5	109.2 ± 14.0
$T_{1/2}$ (h)	1.006 ± 0.143	1.247 ± 0.445	1.056 ± 0.542	1.820 ± 0.581	1.174 ± 0.231	1.030 ± 0.893	1.663 ± 0.175
AUC_{last} (ng·h/mL)	300.9 ± 49.17	902.5 ± 150.3	3375 ± 254.3	44.71 ± 11.05	585.7 ± 86.65	811.5 ± 120.8	213.4 ± 33.78
AUC_{inf} (ng·h/mL)	302.6 ± 48.28	905.0 ± 150.1	3378 ± 254.0	49.88 ± 9.242	589.2 ± 86.29	813.1 ± 122.0	219.6 ± 33.20
CL (mL/(h·kg))	1012 ± 163.8	1130 ± 187.7	892.2 ± 66.86	NC	NC	2496 ± 360	NC
V_{ss} (mL/kg)	303.8 ± 133.2	256.2 ± 59.80	170.7 ± 77.07	NC	NC	661.2 ± 61.7	NC
Bioavailability (%)				5.512 ± 1.021	65.10 ± 9.535	100	0.540 ± 0.082

AUC, area under the plasma concentration–time curve; CL, systemic clearance; C_{max}, peak plasma concentration; NC, not calculated; $T_{1/2}$, terminal elimination half-life; T_{max}, time to reach C_{max}; V_{ss}, steady-state volume of distribution

& editing. **Kyeong-Ryoon Lee:** Formal analysis. **Soo-Jin Kim:** Conceptualization, Methodology, Visualization, Supervision. **Tae-Sung Koo:** Conceptualization, Methodology, Visualization, Supervision. **:** .

Declaration of Competing Interest

The authors declare the following financial interests/personal relationships which may be considered as potential competing interests: THK, GYK, and HJP are an employee of Daewoong Pharmaceuticals, and SJ Kim is an employee of Daewoong Therapeutics Inc., and all other authors declare that there is no conflict of interest.

Acknowledgements

This work was supported by Chungnam National University.

References

[1] Z.Y. Zu, M.D. Jiang, P.P. Xu, W. Chen, Q.Q. Ni, G.M. Lu, L.J. Zhang, Coronavirus disease (COVID-19): a perspective from China, Radiology 296 (2020) (2019) E15–E25, https://doi.org/10.1148/radiol.2020200490.
[2] Q. Wang, Y. Zhang, L. Wu, S. Niu, C. Song, Z. Zhang, G. Lu, C. Qiao, Y. Hu, K.-Y. Yuen, Structural and functional basis of SARS-CoV-2 entry by using human ACE2, Cell 181 (2020) 894–904.e9, https://doi.org/10.1016/j.cell.2020.03.045.
[3] N. Zhu, D. Zhang, W. Wang, X. Li, B. Yang, J. Song, X. Zhao, B. Huang, W. Shi, R. Lu, A novel coronavirus from patients with pneumonia in China, N. Engl. J. Med. 382 (2020) (2019) 727–733, https://doi.org/10.1056/NEJMoa2001017.
[4] T. Singhal, A review of coronavirus disease-2019 (COVID-19), The indian journal of pediatrics 87 (2020) 281–286, https://doi.org/10.1007/s12098-020-03263-6.
[5] E.C. Weinbach, J. GARBUS, Mechanism of action of reagents that uncouple oxidative phosphorylation, Nature 221 (1969) 1016–1018, https://doi.org/10.1038/2211016a0.
[6] R.C. Arend, A.I. Londoño-Joshi, R.S. Samant, Y. Li, M. Conner, B. Hidalgo, R. D. Alvarez, C.N. Landen, J.M. Straughn, D.J. Buchsbaum, Inhibition of Wnt/β-catenin pathway by niclosamide: A therapeutic target for ovarian cancer, Gynecol. Oncol. 134 (2014) 112–120, https://doi.org/10.1016/j.ygyno.2014.04.005.
[7] S. Burock, S. Daum, U. Keilholz, K. Neumann, W. Walther, U. Stein, Phase II trial to investigate the safety and efficacy of orally applied niclosamide in patients with metachronous or sychronous metastases of a colorectal cancer progressing after therapy: the NIKOLO trial, BMC cancer 18 (2018) 1–7, https://doi.org/10.1186/s12885-018-4197-9.
[8] M.B. Monin, P. Krause, R. Stelling, D. Bocuk, S. Niebert, F. Klemm, T. Pukrop, S. Koenig, The anthelmintic niclosamide inhibits colorectal cancer cell lines via modulation of the canonical and noncanonical Wnt signaling pathway, J. Surg. Res. 203 (2016) 193–205, https://doi.org/10.1016/j.jss.2016.03.051.
[9] M.T. Schweizer, K. Haugk, J.S. McKiernan, R. Gulati, H.H. Cheng, J.L. Maes, R. F. Dumpit, P.S. Nelson, B. Montgomery, J.S. McCune, A phase I study of niclosamide in combination with enzalutamide in men with castration-resistant prostate cancer, PLoS ONE 13 (2018), e0198389, https://doi.org/10.1371/journal.pone.0202709.
[10] N.C. Gassen, D. Niemeyer, D. Muth, V.M. Corman, S. Martinelli, A. Gassen, K. Hafner, J. Papies, K. Mösbauer, A. Zellner, SKP2 attenuates autophagy through Beclin1-ubiquitination and its inhibition reduces MERS-Coronavirus infection, Nat. Commun. 10 (2019) 1–16, https://doi.org/10.1038/s41467-019-13659-4.
[11] N.C. Gassen, J. Papies, T. Bajaj, F. Dethloff, J. Emanuel, K. Weckmann, D.E. Heinz, N. Heinemann, M. Lennarz, A. Richter, Analysis of SARS-CoV-2-controlled autophagy reveals spermidine, MK-2206, and niclosamide as putative antiviral therapeutics, BioRxiv (2020), https://doi.org/10.1101/2020.04.15.997254.
[12] C.-J. Wu, J.-T. Jan, C.-M. Chen, H.-P. Hsieh, D.-R. Hwang, H.-W. Liu, C.-Y. Liu, H.-W. Huang, S.-C. Chen, C.-F. Hong, Inhibition of severe acute respiratory syndrome coronavirus replication by niclosamide, Antimicrob. Agents Chemother. 48 (2004) 2693–2696, https://doi.org/10.1128/AAC.48.7.2693-2696.2004.
[13] S. Jeon, M. Ko, J. Lee, I. Choi, S.Y. Byun, S. Park, D. Shum, S. Kim, Identification of antiviral drug candidates against SARS-CoV-2 from FDA-approved drugs, Antimicrobial Agents and Chemotherapy, 64 (2020) e00819-20, https://doi.org/10.1128/AAC.00819-20.
[14] NIH U. S. National Library of Medicine, ClinicalTrials.gov https://www.clinicaltrials.gov/ct2/results?recrs=&cond=COVID-19&term=niclosamide&cntry=&state=&city=&dist= (accessed 07 March 2021).
[15] G. Doran, M.M. Stevens, Simultaneous determination of niclosamide and its degradates in water by LC-MS/MS, Anal. Methods 6 (2014) 6871–6877, https://doi.org/10.1039/C4AY01074D.
[16] H. Jiang, Y. Zhang, X. Chen, J. Lv, J. Zou, Simultaneous determination of pentachlorophenol, niclosamide and fenpropathrin in fishpond water using an LC-MS/MS method for forensic investigation, Anal. Methods 5 (2013) 111–115, https://doi.org/10.1039/C2AY25685A.
[17] Y.-W. Chang, T.-K. Yeh, K.-T. Lin, W.-C. Chen, H.-T. Yao, Pharmacokinetics of anti-SARS-CoV agent niclosamide and its analogs in rats, J. Food Drug Anal. 14 (2006) 329–333, https://doi.org/10.38212/2224-6614.2464.
[18] U.S., Food and Drug Administration, Guidance for Industry, Bioanalytical Method Validation (2018).
[19] European Medicines Agency, Guideline on Bioanalytical Method Validation (2011).
[20] Y.-G. Ji, Y.-M. Shin, J.-W. Jeong, H.-I. Choi, S.-W. Lee, J.-H. Lee, K.-R. Lee, T.-S. Koo, Determination of motolimod concentration in rat plasma by liquid chromatography-tandem mass spectrometry and its application in a pharmacokinetic study, J. Pharm. Biomed. Anal. 179 (2020), 112987, https://doi.org/10.1016/j.jpba.2019.112987.
[21] S.-H. Jeong, J.-H. Jang, H.-Y. Cho, I.-J. Oh, Y.-B. Lee, A sensitive UPLC–ESI–MS/MS method for the quantification of cinnamic acid in vivo and in vitro: application to pharmacokinetic and protein binding study in human plasma, Journal of Pharmaceutical Investigation 50 (2020) 159–172, https://doi.org/10.1007/s40005-019-00444-0.
[22] J. Fan, I.A. de Lannoy, Pharmacokinetics, Biochem Pharmacol 87 (2014) 93–120, https://doi.org/10.1016/j.bcp.2013.09.007.
[23] A.F. El-Kattan, Oral bioavailability assessment: basics and strategies for drug discovery and development, Wiley, 2017, p. 7.